

Light Quark Mediated Higgs Boson Threshold Production in the Next-to-Leading Logarithmic Approximation

Charalampos Anastasiou,^a Alexander Penin^b

^b*Institute for Theoretical Physics, ETH Zürich, 8093 Zürich, Switzerland*

^a*Department of Physics, University of Alberta, Edmonton AB T6G 2J1, Canada*

E-mail: babis@phys.ethz.ch, penin@ualberta.ca

ABSTRACT: We study the amplitude of the Higgs boson production in gluon fusion mediated by a light quark loop and evaluate the logarithmically enhanced radiative corrections to the next-to-leading logarithmic approximation which sums up the terms of the form $\alpha_s^n \ln^{2n-1}(m_H/m_q)$ to all orders in the strong coupling constant. This result is used for the calculation of the process cross section near the production threshold and gives a quantitative estimate of the three and four-loop bottom quark contribution to the Higgs boson production at the Large Hadron Collider.

Contents

1	Introduction	1
2	General structure of the leading and next-to-leading logarithms	2
2.1	Sudakov form factor	3
2.2	Massive quark scattering by a gauge field operator	5
3	$gg \rightarrow H$ amplitude mediated by a light quark	12
4	Higgs boson threshold production	14
4.1	Partonic cross section near the threshold	15
4.2	Hadronic cross section in the threshold approximation	17
5	Conclusion	20

1 Introduction

Accurate theoretical predictions for the (inclusive and differential) Higgs gluon fusion cross section are indispensable for the determination with high precision of the Higgs boson couplings [1]. A dominant component of the gluon fusion process originates from Feynman diagrams with a virtual top quark inside the loop. Due to the hierarchy of the top quark and Higgs boson masses, this component can be accurately determined by expanding around the heavy top quark limit [2–4]. In this approach, where top quark loops are reduced to effective point-like vertices, gluon fusion cross sections are now known precisely at very high orders in perturbative QCD [5–14].

With the achieved precision of a few percent, contributions of lighter quarks of a suppressed Higgs Yukawa coupling cannot be ignored.¹ For light quarks, the top quark effective field theory calculations are inapplicable. The relevant Higgs production probability amplitudes need to be computed with their exact quark mass dependence or, alternatively, by means of a systematic expansion around the antithetic asymptotic limit in which the quark mass is vanishing. The exact quark mass dependence for the $gg \rightarrow H$ amplitude is only known through two loops [15–22]. The two-loop amplitudes for the top-bottom interference in the next-to-leading order cross section [23–25] for the production of a Higgs boson in association with a jet have been computed by means of a small quark mass expansion.

In the small quark mass limit the radiative corrections are enhanced by a power of the logarithm $\ln(m_H/m_q)$ of the Higgs boson to a light quark mass ratio. For the physical values of the bottom and charm quark masses the numerical value of the logarithm is quite large and it is important to control the size of the logarithmic corrections beyond two

¹For a recent estimate of their effect to the inclusive Higgs cross-section see, for example, Ref. [6].

loops. For the $gg \rightarrow H$ amplitude the leading (double) logarithmic corrections have been evaluated to all orders in strong coupling constant α_s in Refs. [26, 27]. The abelian part of the double-logarithmic corrections for the $gg \rightarrow Hg$ amplitude of Higgs plus jet production has been obtained in Ref. [28]. Though the leading logarithmic approximation gives a qualitative estimate of the QCD corrections beyond two loops, subleading logarithmic corrections can be numerically important. Their computation is necessary to quantifying the theoretical uncertainty estimate. In particular, in the leading logarithmic approximation the numerical predictions vary significantly with values of light quark masses being taken in different renormalization schemes. The logarithmic terms sensitive to ultraviolet renormalization, which cancel the dependence of the amplitude on the renormalization scheme, are formally subleading. Extending the analysis beyond the leading logarithmic approximation is therefore highly desired. In this paper, we present the analysis of the light quark loop mediated $gg \rightarrow H$ amplitude in the next-to-leading logarithmic approximation which sums up the terms of the form $\alpha_s^n \ln^{2n-1}(m_H/m_q)$ to all orders in perturbation theory and use this result for the evaluation of the bottom quark effect on the Higgs boson production cross section near the threshold.

The paper is organized as follows. In the next section we discuss the general structure of the leading and next-to-leading logarithmic approximation, derive the factorization and perform the resummation of the next-to-leading logarithmic corrections to a model mass-suppressed amplitude of quark scattering by a scalar gauge field operator. In Sect. 3 we apply the method to the analysis of the $gg \rightarrow Hg$ amplitude mediated by a light quark loop. The result is used in Sect. 4 for the calculation of the bottom quark contribution to the cross section of the Higgs boson production in gluon fusion in the threshold approximation. Sect. 5 is our conclusion.

2 General structure of the leading and next-to-leading logarithms

The logarithmically enhanced contributions under consideration appear in the high-energy or small-mass limit of the on-shell gauge theory amplitudes. To the leading order of the small-mass expansion these are renowned “Sudakov” logarithms which have been extensively studied since the pionering work [29]. The structure of the Sudakov logarithms in the theories with massive fermions and gauge bosons is by now well understood [30–48]. The characteristic feature of the $gg \rightarrow H$ amplitude however is that it vanishes in the limit of the massless quark $m_q \rightarrow 0$ *i.e.* is power-suppressed. The asymptotic behavior of the power suppressed amplitudes may be significantly different from the Sudakov case and attract a lot of attention in many various contexts (see *e.g.* [26–28, 49–78]). At the same time the logarithmically enhanced corrections to the on-shell (or almost on-shell) amplitudes in the high energy limit are universally associated with the emission of the virtual particles which are soft and/or collinear to the large external momenta. It is instructive first to review the origin and the structure of such corrections to the leading-power amplitudes. In the next section we discuss the asymptotic behavior of the quark form factor to the next-to-leading logarithmic approximation, which will be used for the analysis of the Higgs production in Sect. 3.

2.1 Sudakov form factor

We consider the limit of the large Euclidean momentum transfer $Q^2 = -(p_2 - p_1)^2$ and slightly off-shell external Euclidean quark momenta $m_q^2 \ll -p_i^2 \ll Q^2$. In this limit the ‘‘Sudakov’’ radiative corrections enhanced by the logarithm of the small ratio p_i^2/Q^2 are known to exponentiate [29–34] and to the next-to-leading logarithmic approximation the Dirac form factor F_1 of the quark scattering in an external abelian vector field reads

$$F_1^{NLL} = \exp \left\{ -\frac{C_F \alpha_s}{2\pi} I_{DL}(p_1^2, p_2^2, 0) \left[1 - \beta_0 \frac{\alpha_s}{8\pi} \left(\ln \left(\frac{-p_1^2}{\mu^2} \right) + \ln \left(\frac{-p_2^2}{\mu^2} \right) \right) \right] \right. \\ \left. + \gamma_q^{(1)} \frac{\alpha_s}{2\pi} I_{SL}(p_1^2, p_2^2, 0) \right\}, \quad (2.1)$$

where $\beta_0 = \frac{11}{3}C_A - \frac{4}{3}T_F n_l$ is the one-loop beta-function for n_l light flavors, $C_F = (N_c^2 - 1)/(2N_c)$, $C_A = N_c$, $T_F = \frac{1}{2}$ for the $SU(N_c)$ color group, $\alpha_s \equiv \alpha_s(\mu)$ is the strong coupling constant at the renormalization scale μ , $\gamma_q^{(1)} = 3C_F/2$ is the one-loop quark collinear anomalous dimension, and I_{DL} (I_{SL}) is the double (single) logarithmic one-loop virtual momentum integral. Let us consider the evaluation of the above integrals in more detail. The double-logarithmic contribution is generated by the scalar three-point integral

$$I_{DL}(p_1^2, p_2^2, m_q^2) = \frac{iQ^2}{\pi^2} \int \frac{d^4 l}{l^2 ((p_1 - l)^2 - m_q^2) ((p_2 - l)^2 - m_q^2)}, \quad (2.2)$$

where l is the gluon momentum. For $m_q^2 = 0$ the above integral can be computed by using the expansion by regions method [79–81] with the result

$$I_{DL}(p_1^2, p_2^2, 0) = \left[\frac{1}{\varepsilon^2} - \frac{1}{\varepsilon} (\ln Q^2 - \ln(-p_1^2) - \ln(-p_2^2)) + \frac{1}{2} \ln^2 Q^2 \right. \\ \left. - \ln Q^2 (\ln(-p_1^2) + \ln(-p_2^2)) + \ln^2(-p_1^2) + \ln^2(-p_2^2) \right]_{us} \\ + \left[-\frac{2}{\varepsilon^2} + \frac{1}{\varepsilon} (\ln(-p_1^2) + \ln(-p_2^2)) + \frac{1}{2} \ln^2(-p_1^2) + \frac{1}{2} \ln^2(-p_2^2) \right]_c \\ + \left[\frac{1}{\varepsilon^2} - \frac{1}{\varepsilon} \ln Q^2 + \frac{1}{2} \ln^2 Q^2 \right]_h + \dots \\ = \ln \left(\frac{Q^2}{-p_1^2} \right) \ln \left(\frac{Q^2}{-p_2^2} \right) + \dots, \quad (2.3)$$

where the ellipsis stand for the nonlogarithmic terms, $\varepsilon = (d - 4)/2$ is the parameter of dimensional regularization and the contributions of the ultrasoft, collinear and hard regions are given separately (for application of the expansion by regions to the form factor analysis see [38]). Note that the logarithmic contribution can be read off the singularity structure of the ultrasoft and collinear regions where the quark propagators may be taken in the eikonal approximation. As we see the integral I_{DL} generates pure double-logarithmic contribution associated with the overlapping soft and collinear divergences and does not generate any single logarithmic term. On the other hand the double-logarithmic term can be obtained

directly by means of the original Sudakov method [29]. In this case the propagators in Eq. (2.2) are approximated as follows

$$\frac{1}{l^2} \approx -i\pi\delta(Q^2 uv - l_\perp^2), \quad \frac{1}{(p_1 - l)^2} \approx -\frac{1}{Q^2 v}, \quad \frac{1}{(p_2 - l)^2} \approx -\frac{1}{Q^2 u}, \quad (2.4)$$

where we introduce the standard Sudakov parametrization of the soft gluon momentum $l = up_1 + vp_2 + l_\perp$ with Euclidean $l_\perp^2 \geq 0$. The logarithmic scaling of the integrand requires $-p_1^2/Q^2 < |v| < 1$, $-p_2^2/Q^2 < |u| < 1$ and the additional kinematical constraints $uv > 0$ has to be imposed to ensure that the soft gluon propagator can go on the mass shell. After integrating Eq. (2.2) over l_\perp we get

$$\int_{-p_1^2/Q^2}^1 \frac{dv}{v} \int_{-p_2^2/Q^2}^1 \frac{du}{u} = \ln\left(\frac{Q^2}{-p_1^2}\right) \ln\left(\frac{Q^2}{-p_2^2}\right). \quad (2.5)$$

Note that the lower integration limits in Eq. (2.5) are determined in the leading logarithmic approximation only up to a constant factor which we choose in such a way that Eq. (2.5) reproduces the result of the explicit evaluation Eq. (2.2) to the next-to-leading logarithmic accuracy. As it follows from Eq. (2.4) the logarithmic contribution to I_{DL} is saturated by the “soft” virtual momentum² with $l^2 \approx 0$ corresponding to the gluon propagator pole position with the quark propagators carrying the large external momenta being eikonal.

The single-logarithmic one-loop term gets contribution from the part of the vertex diagram linear and quadratic in the virtual gluon momentum as well as from the quark self-energy diagram and can be reduced to the sum of two scalar integrals

$$I_{SL}(p_1^2, p_2^2, m_q^2) = \frac{i}{2\pi^2} \int \frac{d^4 l}{(p_2 - l)^2 - m_q^2} \left(\frac{1}{l^2} - \frac{1}{(p_1 - l)^2 - m_q^2} \right) + (p_1 \leftrightarrow p_2). \quad (2.6)$$

The first integral develops the logarithmic contribution when the virtual momentum becomes collinear to p_1 . In the light-cone coordinates where $p_1 \approx p_1^-$ and $p_2 \approx p_2^+$ it takes the following form

$$\frac{i}{2\pi} \int \frac{dl^+ dl^- dl_\perp^2}{(2p_2^+ l^- - l^2)} \left(\frac{1}{l^2} + \frac{1}{(2p_1^- l^+ - l^2)} \right), \quad (2.7)$$

where we neglected m_q^2 and p_i^2 . The integral over l^- can then be performed by taking the residue of the quark propagator with the external momentum p_2 which gives

$$l^- = \frac{-l_\perp^2}{2(p_2^+ - l^+)} \quad (2.8)$$

with a condition $0 \leq l^+ \leq p_2^+$ on the second light-cone component of the virtual momentum. Then Eq. (2.7) takes the following form

$$\int_0^{p_2^+} \frac{dl^+}{2p_2^+} \int dl_\perp^2 \left(\frac{1}{l_\perp^2} - \frac{1}{l_\perp^2 + Q^2 l^+ (p_2^+ - l^+) / (p_2^+)^2} \right). \quad (2.9)$$

²This should not be confused with the soft momentum region of the expansion by regions approach.

Since $l^+ \sim p^+$ the integral over the transversal component of the virtual momentum is logarithmic for $l_\perp \ll Q$ and is regulated by m_q^2 or $-p_2^2$ at small l_\perp . Thus for $m_q^2 \ll -p_1^2$ with the logarithmic accuracy we get

$$\int_0^{p_2^+} \frac{dl^+}{2p_2^+} \int_{-p_2^2}^{Q^2} \frac{dl_\perp^2}{l_\perp^2} = \frac{1}{2} \ln \left(\frac{Q^2}{-p_1^2} \right) \quad (2.10)$$

and

$$I_{SL}(p_1^2, p_2^2, 0) = \frac{1}{2} \left[\ln \left(\frac{Q^2}{-p_1^2} \right) + \ln \left(\frac{Q^2}{-p_2^2} \right) \right] + \dots \quad (2.11)$$

The β_0 term in the exponent Eq. (2.1) sets the scale of the strong coupling constant in the double-logarithmic contribution and is a geometric average of the hard scale Q^2 and the ultrasoft scale p_i^4/Q^2 , as follows from the evolution equations analysis [37, 38].

For the analysis of the Higgs boson production we need a generalization of the above result to the quark scalar form factor F_S . The structure of the Sudakov logarithms does not depend on the Lorenz structure of the amplitude. However, in contrast to the vector case the scalar form factor has a nonvanishing anomalous dimension. The physical scale for the Yukawa coupling to an external scalar field is given by the momentum transfer which results in an additional dependence of the form factor on Q . Thus to the next-to-leading logarithmic accuracy we have

$$F_S^{NLL} = \left(\frac{\alpha_s(Q)}{\alpha_s(\nu)} \right)^{\gamma_m^{(1)}/\beta_0} \exp \left\{ -\frac{C_F \alpha_s}{2\pi} \ln \left(\frac{Q^2}{-p_1^2} \right) \ln \left(\frac{Q^2}{-p_2^2} \right) \left[1 - \beta_0 \frac{\alpha_s}{8\pi} \left(\ln \left(\frac{-p_1^2}{\mu^2} \right) + \ln \left(\frac{-p_2^2}{\mu^2} \right) \right) \right] + \gamma_q^{(1)} \frac{\alpha_s}{4\pi} \left[\ln \left(\frac{Q^2}{-p_1^2} \right) + \ln \left(\frac{Q^2}{-p_2^2} \right) \right] \right\}, \quad (2.12)$$

where the exponential factor is identical to Eq. (2.1), in the renormalization group factor $\gamma_m^{(1)} = 3C_F$ is the quark mass anomalous dimension, and ν is the renormalization scale of the Yukawa coupling.

The light quark mediated $gg \rightarrow H$ amplitude is suppressed by the quark mass and its high-energy asymptotic behavior is significantly different from the leading-power Sudakov form factor considered above. To determine the structure of the logarithmically enhanced corrections in this case in the next section we consider an auxiliary amplitude of a massive quark scattering by an abelian gauge field operator. This rather artificial amplitude is a perfect toy model which reveals the main features of the problem in the most illustrative way with minimal technical complications and the corresponding analysis can be easily generalized to the other mass-suppressed amplitudes and nonabelian gauge groups.

2.2 Massive quark scattering by a gauge field operator

We consider quark scattering by a local operator $(G_{\mu\nu})^2$ of an abelian gauge field strength tensor for the on-shell initial and final quark momentum $p_1^2 = p_2^2 = m_q^2 \ll Q^2$. A detailed discussion of this process in the leading logarithmic approximation can be found in Refs. [26, 27]. Below we extend the analysis to the next-to-leading logarithmic approximation. The leading order scattering is given by the one-loop diagram in Fig. 1(a). Due to helicity

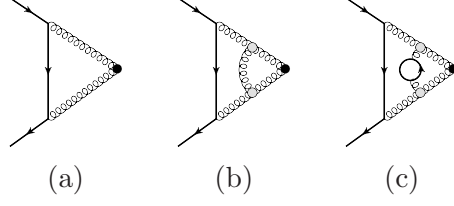


Figure 1. The Feynman diagrams for (a) the leading order one-loop quark scattering by the $(G_{\mu\nu})^2$ vertex (black circle), (b) the soft gauge boson exchange with the effective vertices (gray circles) defined in the text which represents the non-Sudakov double-logarithmic corrections, (c) the renormalization group running of the effective coupling constant in (b).

conservation the corresponding amplitude is suppressed at high energy by the quark mass and with the logarithmic accuracy reads

$$\mathcal{G}^0 = \frac{\alpha_q}{\pi} (I'_{DL}(m_q^2, m_q^2, m_q^2) + 3I'_{SL}(m_q^2, m_q^2, m_q^2) - 3I_{UV}) m_q \bar{q}q, \quad (2.13)$$

where, $\alpha_q = e_q^2/(4\pi)$, e_q is the quark abelian charge and the scalar double-logarithmic integral over the virtual quark momentum reads

$$I'_{DL}(p_1^2, p_2^2, m_q^2) = \frac{iQ^2}{\pi^2} \int \frac{d^4l}{(l^2 - m_q^2)(p_1 + l)^2(p_2 + l)^2}. \quad (2.14)$$

The integral can be evaluated through the expansion by regions with the result

$$\begin{aligned} I'_{DL}(m_q^2, m_q^2, m_q^2) &= \left[-\frac{2}{\varepsilon^2} + \frac{1}{\varepsilon} \ln(Q^2) - \ln m_q^2 \ln^2 Q^2 + \frac{1}{2} \ln^2 m_q^2 \right]_c \\ &\quad + \left[\frac{1}{\varepsilon^2} - \frac{1}{\varepsilon} \ln Q^2 + \frac{1}{2} \ln^2 Q^2 \right]_h + \dots \\ &= \frac{L^2}{2} + \dots, \end{aligned} \quad (2.15)$$

where $L = \ln(Q^2/m_q^2)$ and the ellipsis stand for the nonlogarithmic terms. The single-logarithmic collinear contribution is given by the integral

$$I'_{SL}(p_1^2, p_2^2, m_q^2) = \frac{i}{2\pi^2} \int \frac{d^4l}{(p_2 - l)^2} \left(\frac{1}{l^2 - m_q^2} - \frac{1}{(p_1 - l)^2} \right) + (p_1 \leftrightarrow p_2) = L + \dots, \quad (2.16)$$

and the ultraviolet divergent contribution reads

$$I_{UV} = \frac{i}{\pi^2} \int \frac{d^{4-2\varepsilon}l}{(p_2 - l)^2(p_1 - l)^2} = -\frac{1}{\varepsilon} + \ln\left(\frac{Q^2}{\nu^2}\right) + \dots, \quad (2.17)$$

where ν is the corresponding ultraviolet renormalization scale. For $\nu = m_q$ the linear logarithmic terms in Eq. (2.13) cancel and the renormalized amplitude in the next-to-leading logarithmic approximation takes a simple form

$$\mathcal{G}^0 = \frac{\alpha_q L^2}{2\pi} m_q \bar{q}q. \quad (2.18)$$

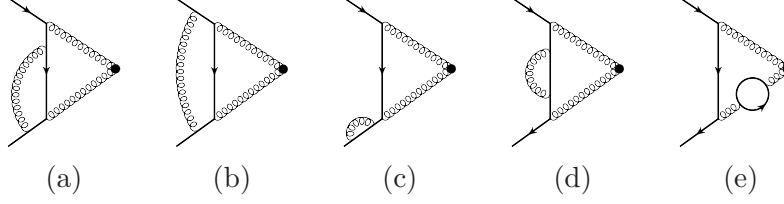


Figure 2. The two-loop Feynman diagrams for the quark scattering by the $(G_{\mu\nu})^2$ vertex (black circle) which contribute in the next-to-leading logarithmic approximation. Symmetric diagrams are not shown.

The integral I'_{DL} in Eq. (2.14) can be evaluated by using the Sudakov parametrization in the same way as it was done in the previous section for I_{DL} . After integrating over l_\perp we get [27]

$$\int_{m_q^2/Q^2}^1 \frac{dv}{v} \int_{m_q^2/vQ^2}^1 \frac{du}{u} = L^2 \int_0^1 d\xi \int_0^{1-\xi} d\eta = \frac{L^2}{2}, \quad (2.19)$$

where the normalized logarithmic variables read $\eta = -\ln v/L$, $\xi = -\ln u/L$. As in Eq. (2.5) we choose the integration limits in such a way that Eq. (2.19) reproduces the result of explicit evaluation Eq. (2.15) to the next-to-leading logarithmic accuracy. A characteristic feature of the mass-suppressed amplitude is that in contrast to the Sudakov form factor the double-logarithmic contribution is generated by a soft quark exchange between the eikonal gauge boson lines. The additional power of m_q originates from the numerator of the virtual quark propagator which effectively becomes scalar and therefore is sufficiently singular at small momentum to provide the double-logarithmic scaling of the one-loop amplitude.

To determine the factorization structure of the next-to-leading logarithms we consider the two-loop radiative corrections and start with the diagrams Fig. 2(a,b), which include all the double-logarithmic contributions. Following Refs. [26, 27] we use a sequence of identities graphically represented in Fig. 3 to move the gauge boson vertex in the diagram Fig. 2(a) from the virtual quark line to an eikonal photon line. Let us describe this procedure in more detail. We choose the virtual momentum routing as shown in Fig. 3(a). To the next-to-leading logarithmic approximation the integration over at least one of the virtual momenta has to be double-logarithmic. We start with the case when this is the virtual quark momentum l , which corresponds to the soft quark $l^2 \sim m_q^2$. The integral over the gauge boson momentum l_g in this case has the same structure as in the one-loop contribution to the vector Sudakov form factor *i.e.* has the double-logarithmic scaling when the gauge boson momentum l_g is soft and the single-logarithmic scaling when l_g is collinear to either p_2 or l . As for the vector form factor the ultraviolet-divergent part of Fig. 3(a) is cancelled against the corresponding ultraviolet-divergent parts of Figs. 2(c,d). Then we can decompose the lower quark propagator as follows

$$S(l + l_g) = S(l + l_g^+) - S(l + l_g) \left(\gamma^+ l_g^- + l_g^\perp \right) S(l + l_g^+). \quad (2.20)$$

The second term in the above equation can be neglected if l_g is collinear to p_2 or soft. In the former case $l_g^- \ll l_g^+$ (*cf.* Eq.(2.8)) while l_g^\perp factor makes the integral over l_g^\perp

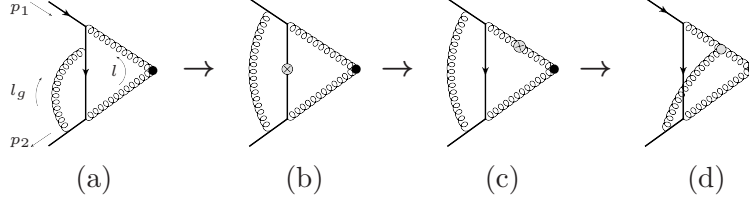


Figure 3. The diagram transformation which moves the gauge boson vertex from the soft quark to the eikonal gauge boson line, as explained in the text.

nonlogarithmic (*cf.* Eq.(2.9)). For soft l_g one has $(l_g^\perp)^2 \sim l_g^- l_g^+$ so the second term in Eq.(2.20) is proportional to l_g^- . Moreover one can neglect l_g^2 in the denominator of the second quark propagator which becomes $S(p_2 + l_g) \sim 1/l_g^-$ and is cancelled by the l_g^- factor so that the integral over l_g depends on $l^2 \sim m_q^2$ and m_q^2 only and does not generate logarithmic corrections. Note that the above approximation is not valid for l_g collinear to l , which will be considered separately. In a covariant gauge only A^- light-cone component of the photon field can be emitted by the eikonal quark line with the momentum p_2 , while the emission of the A^+ and transverse components is suppressed. Thus the interaction of the virtual photon which is soft or collinear to p_2 to the quark line in Fig. 3(a) can be approximated as follows

$$S(l)\gamma^\mu S(l+l_g) \approx S(l)\gamma^- S(l+l_g^+) = \frac{1}{l_g^+} (S(l) - S(l+l_g^+)) . \quad (2.21)$$

which is equivalent to the QED Ward identity. The right hand side of Eq. (2.21) corresponds to the diagram Fig. 3(b) where the crossed circle on the quark propagator represents the replacement $S(l) \rightarrow S(l) - S(l+l_g^+)$ and the $1/l_g^+$ factor is absorbed into the upper eikonal quark propagator. By the momentum shift $l \rightarrow l - l_g^+$ in the second term of the above expression the crossed circle can be moved to the upper eikonal photon line which becomes $\frac{1}{2p_1 l} - \frac{1}{2p_1(l+l_g^+)}$, Fig. 3(c). The opposite eikonal line is not sensitive to this shift since $p_2^- \approx 0$. On the final step we use the “inverted Ward identity” on the upper eikonal gauge boson line

$$\frac{1}{l_g^+} \left(\frac{1}{2p_1 l} - \frac{1}{2p_1(l+l_g^+)} \right) = \frac{1}{2p_1 l} 2p_1^- - \frac{1}{2p_1(l+l_g^+)} \approx \frac{1}{(p_1 - l)^2} 2p_1^\mu \frac{1}{(p_1 - l - l_g)^2} \quad (2.22)$$

to transform the diagram Fig. 3(c) into Fig. 3(d) with an effective dipole coupling $2e_q p_1^\mu$ to the eikonal *gauge boson*, where e_q is the *quark* charge. Note that we can replace $2p_1(l+l_g^+)$ by $-(p_1 - l - l_g)^2$ in the gauge boson propagator as long as $l_g \ll Q$ since $p_1^+ \approx 0$.

Then for the soft virtual momentum l_g one can also use the eikonal approximation for the propagators carrying the external momenta p_i . By adding the symmetric diagram and the diagram Fig. 2(b) we get a “ladder” structure characteristic to the standard eikonal factorization for the Sudakov form factor. This factorization, however, requires the summation over all possible insertions of the soft photon vertex along each eikonal line while in the case under consideration the diagram in Fig. 1(b) with the soft exchange between the

photon lines is missing. This diagram can be added to complete the factorization and then subtracted. After adding the diagram Fig. 1(b) the integral over the soft gauge boson momentum factors out with respect to the leading order amplitude. The additional diagram with effective gauge boson interaction accounts for the variation of the charge propagating along the eikonal lines at the point of the soft quark emission and is characteristic to the leading mass-suppressed amplitudes [26, 27]. At the same time for the virtual momentum collinear to p_2 the eikonal approximation can be used for the propagators carrying the external momentum p_1 while the integration over l_g^- is performed by taking the residue of the $S(p_2 + l_g)$ propagator. Thus the integration over the collinear gauge boson momentum completely factors out in the sum of the diagrams Fig. 2(b) and Fig. 3(d), as well as in the symmetric diagrams contribution when l_g is collinear to p_1 , without any additional subtraction required for the soft virtual momentum. This can be easily understood since in contrast to the soft emission the collinear one is not sensitive to the eikonal charge nonconservation.

In the next-to-leading logarithmic approximation we also need to consider the case when the virtual quark momentum l is either hard or collinear and the corresponding integral is single-logarithmic while the gauge boson momentum l_g is soft and the corresponding integral has double-logarithmic scaling. For hard l the integration over l_g trivially factorizes and is double-logarithmic only for the diagram Fig. 2(b). If l is collinear to p_2 the integral over l_g in the diagram Fig. 2(a) is not double-logarithmic since the soft exchange is between two collinear quark lines. At the same time for l being collinear to p_1 the integral over l_g in this diagram is double-logarithmic but the above algorithm with the momentum shift is not applicable since the upper line gauge boson propagator has to be on-shell. However in this case the diagrams Fig. 2(a,b) already give all possible insertions of the soft gauge boson vertex along the eikonal quark line collinear to p_1 so the integration over the soft momentum l_g also factorizes [82].

The factorized soft and collinear contributions together with the external quark self-energy diagrams Fig. 2(c) add up to the one-loop contribution to the universal factor which describes the next-to-leading Sudakov logarithms for the amplitudes with the quark-antiquark external on-shell lines [36, 38, 41]

$$Z_q^{2NLL} = \exp \left\{ -\frac{\alpha_q}{4\pi} \left[\frac{2}{\varepsilon} \left(\frac{\mu_f^2}{m_q^2} \right)^\varepsilon (1-L) + L^2 \left(1 - \frac{\beta_0}{3} \frac{\alpha_q}{4\pi} L \right) \right] + \gamma_q^{(1)} \frac{\alpha_q}{2\pi} L \right\}, \quad (2.23)$$

where the coupling constant is renormalized at the scale m_q , $\beta_0 = -4/3$ and $\gamma_q^{(1)} = 3/2$ are the corresponding beta-function and the collinear quark anomalous dimension, and the “factorization scale” μ_f is the mass parameter of the dimensional regularization used to deal with the soft divergence not regulated by the quark mass. Hence the next-to-leading logarithmic approximation for the amplitude can be written in the following form

$$\mathcal{G}^{NLL} = Z_q^{2NLL} \left(g(-x) + \frac{\alpha_q L}{4\pi} \Delta_q(-x) \right) \mathcal{G}^{(0)}. \quad (2.24)$$

In this equation the function $g(-x)$ of the variable $x = -\frac{\alpha_q}{4\pi} L^2 < 0$ incorporates the double-logarithmic non-Sudakov contribution of Fig. 1(b) with an arbitrary number of the effective

soft gluon exchanges [27]. It is given by the integral

$$g(x) = 2 \int_0^1 d\xi \int_0^{1-\xi} d\eta e^{2x\eta\xi}, \quad (2.25)$$

where the expression in the exponent is the result of the one-loop integration over the soft gauge boson virtual momentum in Fig. 1(b). The integral can be solved in terms of generalized hypergeometric function

$$g(x) = {}_2F_2(1, 1; 3/2, 2; x/2) = 1 + \frac{x}{6} + \frac{x^2}{45} + \frac{x^3}{420} + \dots \quad (2.26)$$

and has the following asymptotic behavior at $x \rightarrow +\infty$

$$g(x) \sim \left(\frac{2\pi e^x}{x^3} \right)^{1/2}. \quad (2.27)$$

The function $\Delta_q(-x)$ in Eq. (2.24) accounts for the all-order non-Sudakov next-to-leading logarithmic corrections. In two loops these corrections are generated by a part of the collinear contribution which does not factor into Eq. (2.23) and by the renormalization group logarithms proportional to beta-function. Note that to get the next-to-leading two-loop logarithmic contribution the integration over the virtual quark momentum l should be double-logarithmic and we can use the same approximation as for the calculation of the one-loop amplitude. Let us consider the collinear contribution first. As it has been pointed out the contribution of the virtual momentum l_g which is collinear to l in the diagram Fig. 2(a) cannot be factorized into the external quark lines. Since in the double-logarithmic approximation the soft quark momentum is close to the mass shell $l^2 \approx m_q^2$ this contribution can be read off the one-loop result for the Sudakov massive quark form factor with the external on-shell momenta l and p_2 . After adding the symmetric contribution and the self-energy diagram Fig. 2(d) and integrating over l_g we get the factor

$$\gamma_q \frac{\alpha_q}{4\pi} \left[\ln \left(\frac{(lp_1)}{m_q^2} \right) + \ln \left(\frac{(lp_2)}{m_q^2} \right) \right] = \gamma_q^{(1)} \frac{\alpha_q L}{4\pi} (2 - \eta - \xi). \quad (2.28)$$

The renormalization group logarithms from the vacuum polarization of the off-shell eikonal photon propagators in Fig. 2(e) and the symmetric diagram read

$$- \beta_0 \frac{\alpha_q L}{4\pi} (2 - \eta - \xi), \quad (2.29)$$

where we set the renormalization scale of the gauge field operator and α_q in the leading order amplitude to m_q . To get the two-loop cubic logarithms the expressions Eqs. (2.28, 2.29) should be inserted into the integral Eq. (2.25) for $x = 0$ corresponding to the leading order amplitude which gives

$$\Delta_q^{2\text{-loop}} = \frac{4}{3} \left(\gamma_q^{(1)} - \beta_0 \right). \quad (2.30)$$

Since the soft emission from an eikonal line of a given charge factorize and exponentiate, the higher order next-to-leading logarithmic corrections associated with Eqs. (2.28, 2.29)

can be obtained by keeping the exponential factor in the integral Eq. (2.25) unexpanded and the corresponding contribution to Δ_q reads

$$2 \left(\gamma_q^{(1)} - \beta_0 \right) \int_0^1 d\xi \int_0^{1-\xi} d\eta (2 - \eta - \xi) e^{2x\eta\xi} = 2 \left(\gamma_q^{(1)} - \beta_0 \right) (g(x) - g_\gamma(x)) , \quad (2.31)$$

where

$$g_\gamma(x) = \frac{1}{x} \left[\left(\frac{\pi e^x}{2x} \right)^{1/2} \text{erf}(\sqrt{x/2}) - 1 \right] = \frac{1}{3} \left(1 + \frac{x}{5} + \frac{x^2}{35} + \frac{x^3}{315} + \dots \right) \quad (2.32)$$

and $\text{erf}(x)$ is the error function. At $x \rightarrow \infty$ Eq. (2.32) has the following asymptotic behavior

$$g_\gamma(x) \sim \left(\frac{\pi e^x}{2x^3} \right)^{1/2} + \dots \quad (2.33)$$

In three loops, however, a new source of the next-to-leading logarithms starts to contribute, which is related to the renormalization group running of the coupling constant in the diagram with the effective soft gauge boson exchange, Fig. 1(c). This diagram is needed to provide the factorization of the β_0 term in Eq. (3.3). Note that the diagram includes only the soft gauge boson exchange. The expression for the two-loop subdiagram with the vacuum polarization insertion to the soft gauge boson propagator is given up to the overall sign by the result for the two-loop logarithmic corrections proportional to β_0 to the off-shell Sudakov form factor Eq. (2.1) and reads

$$\beta_0 \frac{\alpha_q L}{2\pi} x \eta \xi \left(\frac{L_\mu}{L} - \frac{\eta + \xi}{2} \right) , \quad (2.34)$$

where $L_\mu = \ln(Q^2/\mu^2)$ and μ is the renormalization scale of α_q in the double-logarithmic variable x . As for Eqs. (2.28, 2.29), the corresponding higher order next-to-leading logarithmic corrections are obtained by inserting Eq. (2.34) into the integral Eq. (2.25) which gives

$$-\beta_0 \frac{\alpha_s L}{2\pi} \int_0^1 d\xi \int_0^{1-\xi} d\eta (2x\eta\xi) \left(\frac{L_\mu}{L} - \frac{\eta + \xi}{2} \right) e^{2x\eta\xi} = -\beta_0 \frac{\alpha_s L}{4\pi} g_\beta(x) , \quad (2.35)$$

where we introduced the function

$$\begin{aligned} g_\beta(x) &= \left[\left(\frac{\pi e^x}{2x} \right)^{1/2} \text{erf}(\sqrt{x/2}) - g(x) \right] \frac{L_\mu}{L} + \frac{3}{2x} \left[\left(1 - \frac{x}{3} \right) \left(\frac{\pi e^x}{2x} \right)^{1/2} \text{erf}(\sqrt{x/2}) - 1 \right] \\ &= \left(\frac{x}{6} + \frac{2}{45} x^2 + \frac{x^3}{140} + \dots \right) \frac{L_\mu}{L} - \left(\frac{x}{15} + \frac{2}{105} x^2 + \frac{x^3}{315} + \dots \right) \end{aligned} \quad (2.36)$$

with the following asymptotic behavior at $x \rightarrow \infty$

$$g_\beta(x) \sim \left(\frac{\pi e^x}{2x} \right)^{1/2} \left(\frac{L_\mu}{L} - \frac{1}{2} \right) . \quad (2.37)$$

Note that the leading term of the expansion in $1/x$, Eq. (2.37), vanishes at the normalization scale $\mu = \sqrt{Qm_q}$. The complete next-to-leading logarithmic contribution reads

$$\Delta_q(x) = 2 \left(\gamma_q^{(1)} - \beta_0 \right) (g(x) - g_\gamma(x)) - \beta_0 g_\beta(x). \quad (2.38)$$

We confirm Eq. (2.38) in two-loop approximation through the explicit evaluation of the corresponding Feynman integrals as functions of the quark mass with subsequent expansion of the result in m_q . A detailed discussion of such a calculation will be published elsewhere [83].

Finally we should note that according to Eq. (2.1) the collinear logarithm Eq. (2.28) and the renormalization group logarithm Eq. (2.34) exponentiate while the higher order renormalization group logarithms of the form Eq. (2.29) sum up to the usual running coupling constant factors

$$\left[1 + \beta_0 \frac{\alpha_q L}{4\pi} (1 - \eta) \right]^{-1} \left[1 + \beta_0 \frac{\alpha_q L}{4\pi} (1 - \xi) \right]^{-1}. \quad (2.39)$$

Thus we can rewrite Eq. (2.24) in a more orthodox form

$$\mathcal{G}^{NLL} = 2 \int_0^1 d\xi \int_0^{1-\xi} d\eta \frac{e^{\left\{ -2x\eta\xi \left[1 - \beta_0 \frac{\alpha_q L}{4\pi} \left(\frac{L\mu}{L} - \frac{\eta+\xi}{2} \right) \right] + \gamma_q^{(1)} \frac{\alpha_q L}{4\pi} (2-\eta-\xi) \right\}}}{\left[1 + \beta_0 \frac{\alpha_q L}{4\pi} (1 - \eta) \right] \left[1 + \beta_0 \frac{\alpha_q L}{4\pi} (1 - \xi) \right]} Z_q^{2NLL} \mathcal{G}^{(0)}, \quad (2.40)$$

which would naturally appear within an effective field theory analysis and includes also the terms $\alpha_q^n L^m$ with $m < 2n - 1$. We however prefer to work with the strict logarithmic expansion, Eqs. (2.24, 2.38). These equations reflect the general structure of the non-Sudakov next-to-leading logarithmic corrections and will be generalized to the Higgs boson production in the next section.

3 $gg \rightarrow H$ amplitude mediated by a light quark

The leading order amplitude of the gluon fusion into the Higgs boson is given by the one-loop diagram in Fig. 4(a). The dominant contribution to the process comes from the top quark loop and in the formal limit of the large top quark mass $m_t \gg m_H$ is proportional to the square of the Higgs boson mass m_H . By contrast for a light quark with $m_q \ll m_H$ running inside the loop the amplitude is proportional to m_q^2 . Indeed, the Higgs boson coupling to the quark is proportional to m_q . Then the scalar interaction of the Higgs boson results in a helicity flip at the interaction vertex and helicity conservation requires the amplitude to vanish in the limit $m_q \rightarrow 0$ even if the Higgs coupling to the light quark is kept fixed. By using the explicit one-loop result the light quark mediated amplitude can be written in such a way that its power suppression and the logarithmic enhancement is manifest

$$\mathcal{M}_{gg \rightarrow H}^{q(0)} = -\frac{3}{2} \frac{m_q^2}{m_H^2} L^2 \mathcal{M}_{gg \rightarrow H}^{t(0)}, \quad (3.1)$$

where $L = \ln(-s/m_q^2)$, $s \approx m_H^2$ is the total energy of colliding gluons, and the result is given in terms of the heavy top quark mediated amplitude $\mathcal{M}_{gg \rightarrow H}^{t(0)}$, which corresponds to a local gluon-gluon-Higgs interaction vertex and has one independent helicity component.

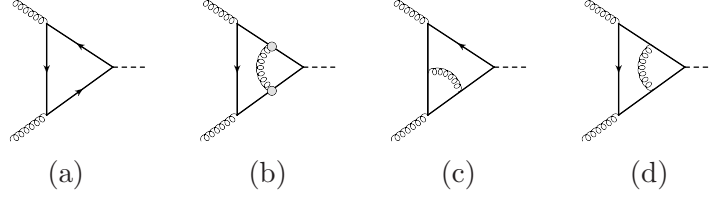


Figure 4. The Feynman diagram for (a) the leading order one-loop Higgs boson production in gluon fusion, (b) the effective soft gauge boson exchange similar to Fig. 1(b), (c) gluon and (d) Higgs boson vertex corrections.

Though apparently completely different, the $gg \rightarrow H$ amplitude shares several crucial properties with the quark scattering amplitude considered in the previous section: it is suppressed by the leading power of the quark mass due to the helicity flip, the double-logarithmic contribution is induced by the soft quark exchange and the (color) charge is not conserved along the eikonal lines. Moreover, since the eikonal (Wilson) lines are characterized by the momentum and color charge but not the spin, the factorization structure of soft and collinear logarithmic corrections described in the Sect. 2.2 directly applies to the case under consideration. In particular the non-Sudakov double-logarithmic corrections are determined by the diagram Fig. 4(b) with the effective soft gluon exchange and are described by the same function $g(x)$ with $x = (C_A - C_F)\frac{\alpha_s}{4\pi}L^2 > 0$, where the color factor accounts for the eikonal color charge variation and the opposite sign of the argument is dictated by the direction of the color flow.³ Thus the next-to-leading factorization formula for the amplitude takes the following form (*cf.* Eq. (2.24))

$$\mathcal{M}_{gg \rightarrow H}^{qNLL} = Z_g^{2NLL} \left(g(x) + \frac{\alpha_s L}{4\pi} \Delta_g(x) \right) \left(\frac{\alpha_s(m_H)}{\alpha_s(m_q)} \right)^{\gamma_m^{(1)}/\beta_0} \mathcal{M}_{gg \rightarrow H}^{q(0)}, \quad (3.2)$$

where the Sudakov factor for a gluon scattering is (see *e.g.* [84])

$$Z_g^{2NLL} = \exp \left[-\frac{\alpha_s}{4\pi} \left(\frac{2C_A}{\varepsilon^2} + \frac{\beta_0}{\varepsilon} \right) \left(\frac{s}{\mu^2} \right)^{-\varepsilon} + \mathcal{O}(\alpha_s^2) \right], \quad (3.3)$$

and we renormalize the strong coupling constant in the leading order amplitude at the infrared factorization scale $\mu_f = \mu$. The extra renormalization group factor appears in Eq. (3.2) since the leading order amplitude is defined in terms of the quark pole mass while the physical renormalization scale of the quark Yukawa coupling is m_H .

As for the quark scattering amplitude, the next-to-leading logarithmic term $\Delta_g(x)$ gets contributions from the collinear gluon exchange which does not factorize into Eq. (3.3) and from the renormalization group running of the coupling constant in the diagram Fig. 4(b) with the effective soft gluon exchange. The latter is identical to Eq. (2.35) up to the definition of x variable and the value of beta-function. The nonfactorizable collinear contribution

³The relation between the double-logarithmic asymptotic behavior of different amplitudes and gauge theories is discussed in detail in Refs. [26, 27]

needs additional analysis though. The diagram which can potentially develop such a contribution can be classified as the corrections to the gluon and Higgs boson vertices with the typical examples given in Fig. 4(c,d). In these diagrams the integral over the soft quark momentum l should be evaluated in the double-logarithmic approximation which effectively put the soft quark on its mass shell $l^2 \approx m_q^2$. The correction to the gluon vertices, Fig. 4(c), with one of the quark lines off-shell by the amount (lp_i) and the corresponding quark self-energy result in a single collinear logarithm

$$\gamma_q \frac{\alpha_q}{4\pi} \left[2 \ln \left(\frac{(p_1 p_2)}{(p_1 l)} \right) + \ln \left(\frac{m_q^2}{(p_1 l)} \right) + (p_1 \leftrightarrow p_2) \right] = \gamma_q^{(1)} \frac{\alpha_q L}{4\pi} (3\eta + 3\xi - 2) . \quad (3.4)$$

Similar contribution associated with the Higgs boson vertex corrections, Fig. 4(d) can be read off the expansion of the Sudakov scalar form factor Eq. (2.12)

$$\gamma_q \frac{\alpha_q}{4\pi} \left[\ln \left(\frac{(p_1 p_2)}{(p_1 l)} \right) + \ln \left(\frac{(p_1 p_2)}{(p_2 l)} \right) \right] = \gamma_q^{(1)} \frac{\alpha_q L}{4\pi} (\eta + \xi) . \quad (3.5)$$

Note that the renormalization group running of the scalar coupling has already been taken into account in the factorization formula Eq. (3.2). To get the corresponding all-order corrections the sum of Eqs. (3.4,3.5) should be inserted into the integral representation of the function $g(z)$ which gives the following contribution⁴ to Δ_g

$$2\gamma_q^{(1)} \int_0^1 d\xi \int_0^{1-\xi} d\eta (4\eta + 4\xi - 2) e^{2x\eta\xi} = 2\gamma_q^{(1)} (4g_\gamma(x) - g(x)) . \quad (3.6)$$

Thus the total result for the next-to-leading logarithmic contribution to the amplitude reads

$$\Delta_g(x) = 2\gamma_q^{(1)} (4g_\gamma(x) - g(x)) - \beta_0 g_\beta(x) \quad (3.7)$$

with the following perturbative expansion

$$\begin{aligned} \Delta_g(x) = C_F \left(1 + \frac{3}{10}x + \frac{x^2}{21} + \dots \right) - \beta_0 \left[\left(\frac{x}{6} + \frac{2}{45}x^2 + \dots \right) \frac{L_\mu}{L} \right. \\ \left. - \left(\frac{x}{15} + \frac{2}{105}x^2 + \dots \right) \right] , \end{aligned} \quad (3.8)$$

where $L_\mu = \ln(-s/\mu^2)$ and the functions $g_\gamma(x)$ and $g_\beta(x)$ are defined by Eq. (2.32) and Eq. (2.36), respectively. In the above equation the three-loop contribution proportional to the beta-function vanishes when the strong coupling constant in the double-logarithmic variable x is renormalized at the scale $\mu = m_H (m_q/m_H)^{2/5}$, which can be considered as the “optimal” renormalization scale in this case.

4 Higgs boson threshold production

The perturbative analysis of the total cross section of the Higgs boson production requires the inclusion of the real emission contribution, which is not yet available for the light quark

⁴The nonabelian gauge interaction does not affect the factorization and exponentiation of the double logarithmic contribution [85].

loop mediated process with arbitrary energy of the emitted partons beyond the next-to-leading order approximation. However, near the production threshold where $z = m_H^2/s \rightarrow 1$ only the soft real emission contributes to the inclusive cross section. For $1 - z \ll m_b/m_H$ the energy of an emitted gluon E_g is much less than m_b . Up to the corrections suppressed by $E_g/m_b \ll 1$ such emission does not resolve the bottom quark loop and has the same structure as in the top quark loop mediated process, where it is known through the next-to-next-to-leading order. Thus we can apply our result for the analysis of the higher order corrections to the Higgs boson threshold production.

4.1 Partonic cross section near the threshold

The expansion of Eqs. (3.2,3.7) gives

$$\mathcal{M}_{gg \rightarrow H}^b = C_b Z_g^2 \left(\frac{\alpha_s(m_H)}{\alpha_s(m_b)} \right)^{\gamma_m^{(1)}/\beta_0} \mathcal{M}_{gg \rightarrow H}^{b(0)}, \quad (4.1)$$

where $C_b = 1 + \sum_{n=1}^{\infty} c_n$ and up to four loops in the next-to-leading logarithmic approximation we get⁵

$$\begin{aligned} c_1 &= \frac{x}{6} + C_F \frac{\alpha_s L}{4\pi}, \\ c_2 &= \frac{x^2}{45} + \frac{x}{5} \frac{\alpha_s L}{4\pi} \left[\frac{3}{2} C_F - \beta_0 \left(\frac{5}{6} \frac{L_\mu}{L} - \frac{1}{3} \right) \right], \\ c_3 &= \frac{x^3}{420} + \frac{x^2}{5} \frac{\alpha_s L}{4\pi} \left[\frac{5}{21} C_F - \beta_0 \left(\frac{2}{9} \frac{L_\mu}{L} - \frac{2}{21} \right) \right]. \end{aligned} \quad (4.2)$$

The coefficient c_1 agrees with the small-mass expansion of the exact two-loop result (see *e.g.* [19]). The higher-order leading logarithmic terms have been obtained in Refs. [26, 27] while the next-to-leading logarithmic terms are new. The n_l part of the β_0 term in the coefficient c_2 agrees with the small-mass expansion of the analytical three-loop result [86].

The three-loop leading logarithmic term has been recently confirmed through numerical calculation [87]. Eq. (4.2) corresponds to the coefficient $(C_A - C_F)^2/5760$ of the L_s^6/z term in Eq. (C.1) of [87], which agrees with the numerical value 0.0004822530864 given in this paper. The three-loop next-to-leading logarithmic term however depends on the ultraviolet renormalization and infrared subtraction scheme. We keep the bottom quark as an active flavor since it contributes to the running of the strong coupling constant in the relevant scale interval $m_b < \mu < m_H$. At the same time in Ref. [87] a massive quark is treated separately and is decoupled even for $m_q \ll m_H$. This changes the running of the effective coupling constant as well as the form of the infrared divergent factor Eq. (3.3) and makes the comparison of the results not quite straightforward beyond the leading logarithmic approximation. As far as we can conclude the conversion of Eq. (4.2) to the scheme used in [87] gives the coefficient $(C_A - C_F)(11C_A/9 - C_F - 10T_F/3)/640$ of the L_s^5/z term in Eq. (C.1), which is in agreement with the numerical value 0.001736111111 obtained in

⁵Since the imaginary part of the amplitude does not contribute to the cross section in the next-to-leading logarithmic approximation we neglect the imaginary part of the logarithms and define $L = \ln(m_H^2/m_b^2)$, $L_\mu = \ln(m_H^2/\mu^2)$ in the rest of the paper

[87]. The mass dependence of the three-loop amplitude has been also studied by numerical method based on conformal mapping and Padé approximants in Ref. [88] but the accuracy of this method in the small-mass limit is not sufficient for a comparison with our result.

The dominant contribution to the cross section is due to the interference of $\mathcal{M}_{gg \rightarrow H}^b$ with the top quark loop mediated amplitude. We can define the nonlogarithmic part of the gluon Sudakov factor Z_g^2 in such a way that it coincides with the gluon form factor which accounts for the virtual corrections to the $gg \rightarrow H$ amplitude in the heavy top quark effective theory. After combining it with the soft real emission we get the known effective theory expression for the radiative corrections to the top quark loop mediated threshold cross section. Then we can write the above top-bottom interference contribution in the factorized form

$$\delta\sigma_{gg \rightarrow H+X}(s) = -3 \frac{m_b^2}{m_H^2} \left(\frac{\alpha_s(m_H)}{\alpha_s(m_b)} \right)^{\gamma_m^{(1)}/\beta_0} L^2 C_b C_t \sigma_{gg \rightarrow H+X}^{\text{eff}}. \quad (4.3)$$

In Eq. (4.3) m_b is the bottom quark pole mass, the heavy top quark effective theory Wilson coefficient for $N_c = 3$ reads [89–91]

$$C_t = 1 + \frac{11}{4} \frac{\alpha_s}{\pi} + \left(\frac{\alpha_s}{\pi} \right)^2 \left[\frac{2777}{288} - \frac{19}{16} \ln \left(\frac{m_t^2}{\mu^2} \right) - n_l \left(\frac{67}{96} + \frac{1}{3} \ln \left(\frac{m_t^2}{\mu^2} \right) \right) \right] + \dots, \quad (4.4)$$

where α_s is the $\overline{\text{MS}}$ coupling constant renormalized at the scale μ , and the effective theory threshold cross section has the following perturbative expansion

$$\sigma_{gg \rightarrow H+X}^{\text{eff}} = \frac{\pi}{v^2(N_c^2 - 1)^2} \left(\frac{\alpha_s}{3\pi} \right)^2 \sum_{n=0}^{\infty} \left(\frac{\alpha_s}{\pi} \right)^n \sigma_n, \quad (4.5)$$

where $v \approx 246$ GeV is the vacuum expectation value of the Higgs field. The coefficients of the expansion Eq. (4.5) are the same as for the top quark loop mediated threshold cross section. The corresponding expressions in terms of delta- and plus-distributions up to $n = 2$ for $N_c = 3$ and the factorization scale $\mu_f = \mu$ read [92, 93]

$$\begin{aligned} \sigma_0 &= \delta(1-z), \\ \sigma_1 &= 6\zeta_2 \delta(1-z) + 6L_\mu \left[\frac{1}{1-z} \right]_+ + 12 \left[\frac{\log(1-z)}{1-z} \right]_+, \\ \sigma_2 &= \delta(1-z) \left\{ \frac{837}{16} + \frac{67}{2} \zeta_2 - \frac{165}{4} \zeta_3 - \frac{9}{8} \zeta_4 + \left(-\frac{27}{2} - \frac{33}{2} \zeta_2 + \frac{171}{2} \zeta_3 \right) L_\mu - 18\zeta_2 L_\mu^2 \right. \\ &\quad + n_l \left[-\frac{247}{36} - \frac{5}{3} \zeta_2 + \frac{5}{6} \zeta_3 + \left(\frac{11}{6} + \zeta_2 \right) L_\mu \right] \left. \right\} + \left[\frac{1}{1-z} \right]_+ \left[-\frac{101}{3} + 33\zeta_2 + \frac{351}{2} \zeta_3 \right. \\ &\quad + \left(\frac{67}{2} - 45\zeta_2 \right) L_\mu - \frac{33}{4} L_\mu^2 + n_l \left(\frac{14}{9} - 2\zeta_2 - \frac{5}{3} L_\mu + \frac{1}{2} L_\mu^2 \right) \left. \right] \\ &\quad + \left[\frac{\log(1-z)}{1-z} \right]_+ \left[67 - 90\zeta_2 - 33L_\mu + 36L_\mu^2 + n_l \left(-\frac{10}{3} + 2L_\mu \right) \right] \\ &\quad + \left[\frac{\log^2(1-z)}{1-z} \right]_+ (-33 + 108L_\mu + 2n_l) + 72 \left[\frac{\log^3(1-z)}{1-z} \right]_+, \end{aligned} \quad (4.6)$$

where $\zeta_n = \zeta(n)$ is a value of Riemann zeta-function. Though Eq. (4.6) includes terms beyond the next-to-leading logarithmic accuracy we prefer to keep them since the logarithmic expansions for c_n and σ_n are of quite different nature. Note that in the effective theory cross section Eq. (4.5) we can take the massless bottom quark limit and in Eq. (4.6) the number of active flavors is $n_l = 5$. By re-expanding Eq. (4.3) in α_s we get the next-to-leading logarithmic result for the leading order (LO), next-to-leading order (NLO), and the next-to-next-to-leading order (NNLO) contributions

$$\begin{aligned}\delta\sigma_{gg\rightarrow H+X}^{\text{NLL, LO}} &= N\sigma_0, \\ \delta\sigma_{gg\rightarrow H+X}^{\text{NLL, NLO}} &= N\left[\left(c_1 - 3C_F\frac{\alpha_s(\nu)L_\nu}{4\pi}\right)\sigma_0 + \frac{\alpha_s}{\pi}\sigma_1\right], \\ \delta\sigma_{gg\rightarrow H+X}^{\text{NLL, NNLO}} &= N\left\{\left[c_2 - C_F\frac{\alpha_s(\nu)L_\nu}{4\pi}\frac{x}{2}\right]\sigma_0 + \frac{\alpha_s}{\pi}\left[c_1 - 3C_F\frac{\alpha_s(\nu)L_\nu}{4\pi}\right]\sigma_1 + \left(\frac{\alpha_s}{\pi}\right)^2\sigma_2\right\},\end{aligned}\tag{4.7}$$

where $L_\nu = \ln(m_H^2/\nu^2)$, the normalization factor is

$$N = -\frac{C_t}{3\pi}\frac{y_b(\nu)}{y_b(m_b)}\left(\frac{\alpha_s L m_b}{(N_c^2 - 1)\nu m_H}\right)^2,\tag{4.8}$$

$y_b(\nu)$ is the bottom quark Yukawa coupling renormalized at the scale ν , and we use the expansion

$$\left(\frac{\alpha_s(m_H)}{\alpha_s(m_b)}\right)^{\gamma_m^{(1)}/\beta_0} = \frac{y_b(\nu)}{y_b(m_b)}\left[1 - 3C_F\frac{\alpha_s(\nu)L_\nu}{4\pi} + \dots\right].\tag{4.9}$$

The expression for the next-to-next-to-next-to-leading order (N³LO) contribution is rather cumbersome and can be obtained from Eq. (4.3) by using our result for c_3 and the N³LO threshold cross-section from [94].

4.2 Hadronic cross section in the threshold approximation

With the partonic result from the previous section we can estimate the bottom quark loop contribution to the hadronic cross section given by

$$\delta\sigma_{pp\rightarrow H+X} = \int dx_1 dx_2 f_g(x_1) f_g(x_2) \delta\sigma_{gg\rightarrow H+X}(x_1 x_2 s),\tag{4.10}$$

where $f_g(x_i)$ is the gluon distribution function and s denotes the square of the partonic center-of-mass energy. In addition to the expressions of the last subsection, as numerical input, we use the hadronic cross section coefficients for top quark contributions in the infinite mass limit evaluated in the threshold approximation through N³LO as obtained by `ihixs2` [95].

The numerical results for the top-bottom interference contribution to the cross section in different orders in α_s are presented in Table 1 for the following values of input parameters: $\alpha_s(M_Z) = 0.118$, $n_l = 5$, $\nu = \mu_f = \mu = m_H/2$, $\overline{m}_b(\overline{m}_b) = 4.18$ GeV, $m_H = 125$ GeV. The above choice of μ ensures a good convergence of the series Eq. (4.5) for $\sigma_{gg\rightarrow H+X}^{\text{eff}}$ [6]. At the same time $\sigma_{gg\rightarrow H+X}^{\text{eff}}$ and C_b in Eq. (4.3) are separately renormalization group invariant

	LO	NLO	NNLO	N ³ LO
$\delta\sigma_{pp\rightarrow H+X}^{\text{LL}}$	-1.420	-1.640	-1.667	-1.670
$\delta\sigma_{pp\rightarrow H+X}^{\text{NLL}}$	-1.420	-2.048	-2.183	-2.204
$\delta\sigma_{pp\rightarrow H+X}$	-1.023	-2.000		

Table 1. The bottom quark loop corrections in picobarns to the Higgs boson production cross section of different orders in α_s given in the leading logarithmic approximation (LL), the next-to-leading logarithmic approximation (NLL) and with full dependence on m_b . All the results are obtained with the threshold partonic cross section at center of mass energy of 13 TeV and renormalization/factorization scales set equal to *half* the Higgs boson mass. Following the conventions of Ref. [6], we use the values of the top and bottom quark Yukawa couplings in the $\overline{\text{MS}}$ -scheme. Our input values at $\mu = m_H/2$ are $\overline{m}_b(\mu) = 2.961$ GeV and $\alpha_s(m_H/2) = 0.1252$. The top quark mass is set to a very large value.

and in general one can use a different value of μ in the series for C_b , Eq. (4.2). However, the corresponding optimal value $\mu = m_H (m_b/m_H)^{2/5} \approx m_H/3$ is quite close to the one for $\sigma_{gg\rightarrow H+X}^{\text{eff}}$ and therefore we use the same renormalization scale in both series. Note that in the NLL approximation there is no difference between the pole mass m_b and the $\overline{\text{MS}}$ mass $\overline{m}_b(\overline{m}_b)$ and we use the latter as the bottom quark mass parameter for its better perturbative properties.

In Table 1 we also present the result obtained with the threshold partonic cross section retaining full dependence on m_b , which is available up to NLO, and the leading logarithmic result obtained with the same σ_n coefficients but all the subleading terms in Eqs. (4.2,4.9) being neglected. As we see, both perturbative and logarithmic expansions have a reasonable convergence. In LO and NLO, where the full mass dependence is known, we find that the NLL cross section is within 42% and 3% of the exact result, respectively. The inclusion of the NLL terms is crucial for reducing the scale dependence as it determines the scales of the bottom quark mass, Yukawa coupling and the strong coupling constant in the LL result. For example, the renormalization group invariant product of the Yukawa factor Eq. (4.9) and the coefficient C_b in NNLO is decreased by about 17% with the scale variation from $m_H/3$ to $2m_H$ in the LL approximation and only by about 5% in the NLL one. The scale dependence of the different orders of perturbative expansion for the threshold cross section in the NLL approximation is shown in Fig. 5.

We should emphasize that the results in Table 1 and Fig. 5 are obtained in the threshold limit. As discussed, for example, in Ref. [57], threshold corrections are not uniquely defined for the hadronic cross section integral. Diverse definitions lead to important numerical differences in the estimate of the cross section. In this paper we have adopted the simplest choice of a flux for the partonic cross section which is given by Eq. (4.10). For top quark contribution only, with the same flux choice, the threshold N³LO cross section in the infinite top quark mass limit constitutes $\sim 65\%$ of the full cross section. While the threshold contribution may not be adequate for precise estimate of the cross section, it does constitute a physical quantity (in contrast to infrared divergent amplitudes) and can therefore be used to detect whether the large logarithms pose any challenges for the convergence of

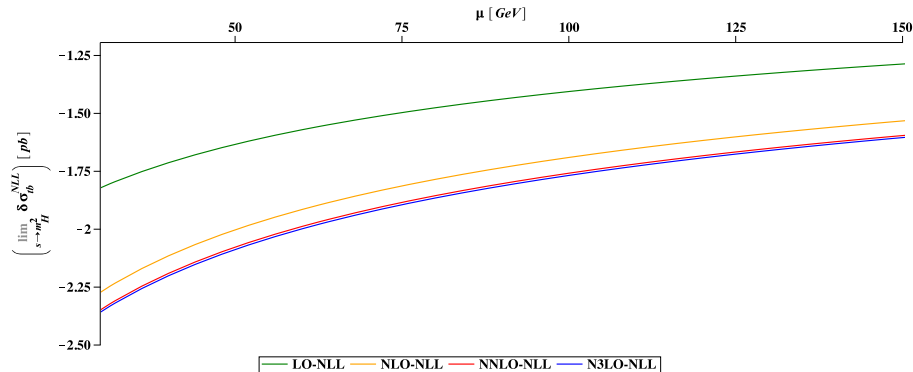


Figure 5. The scale dependence of the top-bottom interference contribution to the threshold cross section in the NLL approximation. The factorization scale and the renormalization scales of the bottom quark Yukawa coupling and the strong coupling constant are set equal $\mu_f = \nu = \mu$. The bottom quark mass, other than in the Yukawa coupling, is set equal to $\overline{m}_b(\overline{m}_b)$. This is a natural choice and differs from the one in Table 1 where for purposes of comparison with prior literature we used $\overline{m}_b(\mu)$ universally.

the perturbative expansion. From the above numerical results we conclude that while in NLO the subleading logarithms are sizable, beyond NLO the logarithmically enhanced corrections are modest and under control.

In Fig. 6 we plot the ratios of the NNLO and N³LO top-bottom interference contribution to the threshold cross section to the NLO result in the NLL approximation. For a wide range of scales the K-factors are in the interval from 1.03 to 1.04. To get an estimate of the total NNLO correction to the bottom quark contribution we can apply the corresponding NLL K-factor to the NLO result with full dependence on m_b which gives

$$\left(\frac{\delta\sigma_{gg \rightarrow H+X}^{\text{NLL, NNLO}}}{\delta\sigma_{gg \rightarrow H+X}^{\text{NLL, NLO}}} - 1 \right) \delta\sigma_{gg \rightarrow H+X}^{\text{NLO}} \approx -0.13 \text{ pb}, \quad (4.11)$$

where we use the numerical values from Table 1. Similar procedure gives the N³LO correction of -0.02 pb .

The accuracy of the NLL approximation in LO and NLO is rather good. For a rough estimate of its accuracy in NNLO we can use the sum of the (highly scheme dependent!) subleading L_s^n/z three-loop terms with $n = 0, \dots, 4$ in Eq. (C.1) of [87]. By applying the corresponding K-factor to the LO result $\delta\sigma_{pp \rightarrow H+X}$ in Table 1 we get a correction of 0.049 pb , which constitutes approximately -40% of the NLL correction Eq. (4.11), very much like for the LO terms. This tempts us to assign in general a 40% uncertainty to the NLL approximation. However, the analysis of the electroweak Sudakov logarithms [39, 41] quite similar to the mass logarithms discussed in this paper suggests that in NNLO the next-to-next-to-leading logarithms can be numerically equal to the LL and the NLL terms. This gives us a conservative estimate of 100% uncertainty of the result Eq. (4.11). Assuming also 15% uncertainty due to the N³LO and higher order corrections together

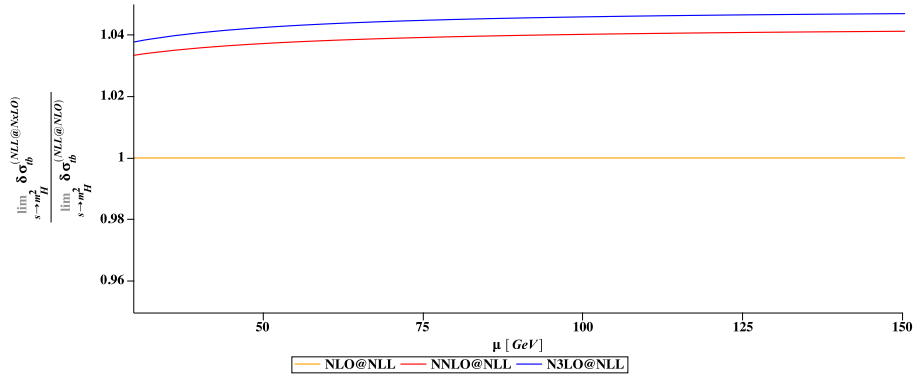


Figure 6. The scale dependence of the ratio of the top-bottom interference contribution to the threshold cross section to the NLO result through N³LO in the NLL approximation. The factorization scale and the renormalization scales of the bottom quark Yukawa coupling and the strong coupling constant are set equal $\mu_f = \nu = \mu$. The bottom quark mass, other than in the Yukawa coupling, is set equal to $\overline{m}_b(\overline{m}_b)$.

with the 50% uncertainty of the threshold approximation discussed above and adding up the errors linearly we obtain a rough estimate of the bottom quark mediated contribution to the total cross section of Higgs boson production in gluon fusion beyond NLO to be in the range from -0.34 to 0.08 *pb*. This falls within a more conservative estimate of ± 0.40 *pb* given in [6] on the basis of the K-factor for the top quark mediated cross section and the scheme dependence of the result. The above interval can be further reduced by evaluating the next-to-next-to-leading logarithmic contribution and getting an approximation valid beyond the threshold region. The latter however requires the analysis of the logarithmically enhanced corrections to the hard real emission which currently is not available even in the LL approximation.

5 Conclusion

We have derived the all-order next-to-leading logarithmic approximation for the light quark loop mediated amplitude of Higgs boson production in gluon fusion. To our knowledge this is the first example of the subleading logarithms resummation for a power-suppressed QCD amplitude. By using this result an estimate of the high-order bottom quark contribution to the Higgs boson production cross section has been obtained in threshold approximation. Despite a large value of the effective expansion parameter $L^2\alpha_s \approx 40\alpha_s$ the corresponding perturbative series does converge. In NLO the next-to-leading logarithmic approximation is in a quite good agreement with the known complete result. For the yet unknown NNLO and N³LO corrections we have obtained -0.13 *pb* and -0.02 *pb*, respectively. With a rather conservative assessment of accuracy of the next-to-leading logarithmic and the threshold approximations we give a rough estimate of the bottom quark mediated contribution to the total cross section of Higgs boson production in gluon fusion beyond NLO to be in the range from -0.34 to 0.08 *pb*.

The actual accuracy of the logarithmic and threshold approximations however is difficult to estimate and an exact computation of quark mass effects is therefore expected to be important in consolidating the theoretical precision of the top-bottom interference contribution to the inclusive Higgs cross section. With the computation of the complete three-loop $gg \rightarrow H$ amplitude in Ref. [87] and recent advances for two-loop $pp \rightarrow H + jet$ amplitudes [96] an exact NNLO result is within reach.

Acknowledgments

C.A is grateful to Achilleas Lazopoulos for his help in producing numerical results with `ihixs2` [95] and to Nicolas Deutschmann and Armin Schweitzer for numerous discussions and comparisons of calculations for the purposes of Ref. [83]. A.P. would like to thank Thomas Becher and Tao Liu for useful communications. The work of A.P. is supported in part by NSERC and Perimeter Institute for Theoretical Physics. The authors thank the Pauli Centre of ETH Zurich for its financial support via its visitors programme.

Note added. In a previous version of this article the contribution of Eq. (3.4) has been omitted. After including this contribution the abelian part of our result agrees with the results [97–99] for the Higgs boson two-photon decay amplitude. The numerical impact of this contribution on the threshold cross-section at NNLO and N³LO is very small.

References

- [1] M. Cepeda *et al.* [HL/HE WG2 group], arXiv:1902.00134 [hep-ph].
- [2] R. V. Harlander, H. Mantler, S. Marzani and K. J. Ozeren, Eur. Phys. J. C **66**, 359 (2010).
- [3] A. Pak, M. Rogal and M. Steinhauser, JHEP **1002**, 025 (2010).
- [4] R. V. Harlander and K. J. Ozeren, JHEP **0911**, 088 (2009).
- [5] C. Anastasiou, C. Duhr, F. Dulat, F. Herzog and B. Mistlberger, Phys. Rev. Lett. **114**, 212001 (2015).
- [6] C. Anastasiou, C. Duhr, F. Dulat, E. Furlan, T. Gehrmann, F. Herzog, A. Lazopoulos and B. Mistlberger, JHEP **1605**, 058 (2016).
- [7] B. Mistlberger, JHEP **1805**, 028 (2018).
- [8] A. Banfi, F. Caola, F. A. Dreyer, P. F. Monni, G. P. Salam, G. Zanderighi and F. Dulat, JHEP **1604**, 049 (2016).
- [9] X. Chen, J. Cruz-Martinez, T. Gehrmann, E. W. N. Glover and M. Jaquier, JHEP **1610**, 066 (2016).
- [10] F. Caola, K. Melnikov and M. Schulze, Phys. Rev. D **92**, 074032 (2015).
- [11] X. Chen, T. Gehrmann, E. W. N. Glover and M. Jaquier, Phys. Lett. B **740**, 147 (2015).
- [12] F. Dulat, B. Mistlberger and A. Pelloni, JHEP **1801**, 145 (2018).
- [13] F. Dulat, B. Mistlberger and A. Pelloni, Phys. Rev. D **99**, 034004 (2019).
- [14] L. Cieri, X. Chen, T. Gehrmann, E. W. N. Glover and A. Huss, JHEP **1902**, 096 (2019).

- [15] D. Graudenz, M. Spira and P. M. Zerwas, Phys. Rev. Lett. **70**, 1372 (1993).
- [16] A. Djouadi, M. Spira and P. M. Zerwas, Phys. Lett. B **264**, 440 (1991).
- [17] M. Spira, A. Djouadi, D. Graudenz and P. M. Zerwas, Nucl. Phys. B **453**, 17 (1995).
- [18] R. Harlander and P. Kant, JHEP **0512**, 015 (2005).
- [19] U. Aglietti, R. Bonciani, G. Degrassi and A. Vicini, JHEP **0701**, 021 (2007).
- [20] R. Bonciani, G. Degrassi and A. Vicini, JHEP **0711**, 095 (2007).
- [21] C. Anastasiou, S. Beerli, S. Bucherer, A. Daleo and Z. Kunszt, JHEP **0701**, 082 (2007).
- [22] C. Anastasiou, S. Bucherer and Z. Kunszt, JHEP **0910**, 068 (2009).
- [23] K. Melnikov, L. Tancredi and C. Wever, JHEP **1611**, 104 (2016).
- [24] K. Melnikov, L. Tancredi and C. Wever, Phys. Rev. D **95**, 054012 (2017).
- [25] J. M. Lindert, K. Melnikov, L. Tancredi and C. Wever, Phys. Rev. Lett. **118**, 252002 (2017).
- [26] T. Liu and A. A. Penin, Phys. Rev. Lett. **119**, 262001 (2017).
- [27] T. Liu and A. Penin, JHEP **1811**, 158 (2018).
- [28] K. Melnikov and A. Penin, JHEP **1605**, 172 (2016).
- [29] V. V. Sudakov, Sov. Phys. JETP **3**, 65 (1956) [Zh. Eksp. Teor. Fiz. **30**, 87 (1956)].
- [30] J. Frenkel and J. C. Taylor, Nucl. Phys. B **116**, 185 (1976).
- [31] A. V. Smilga, Nucl. Phys. B **161**, 449 (1979).
- [32] A. H. Mueller, Phys. Rev. D **20**, 2037 (1979).
- [33] J. C. Collins, Phys. Rev. D **22**, 1478 (1980).
- [34] A. Sen, Phys. Rev. D **24**, 3281 (1981).
- [35] G. F. Sterman, Nucl. Phys. B **281**, 310 (1987).
- [36] G. P. Korchemsky, Phys. Lett. B **217**, 330 (1989).
- [37] G. P. Korchemsky, Phys. Lett. B **220**, 629 (1989).
- [38] J. H. Kuhn, A. A. Penin and V. A. Smirnov, Eur. Phys. J. C **17**, 97 (2000).
- [39] J. H. Kuhn, S. Moch, A. A. Penin and V. A. Smirnov, Nucl. Phys. B **616**, 286 (2001),
Erratum: [Nucl. Phys. B **648**, 455 (2003)].
- [40] B. Feucht, J. H. Kuhn, A. A. Penin and V. A. Smirnov, Phys. Rev. Lett. **93**, 101802 (2004).
- [41] B. Jantzen, J. H. Kühn, A. A. Penin and V. A. Smirnov, Nucl. Phys. B **731**, 188 (2005).
- [42] A. A. Penin, Phys. Rev. Lett. **95**, 010408 (2005).
- [43] A. A. Penin, Nucl. Phys. B **734**, 185 (2006).
- [44] R. Bonciani, A. Ferroglia, and A. A. Penin, Phys. Rev. Lett. **100**, 131601 (2008).
- [45] R. Bonciani, A. Ferroglia, and A. A. Penin, JHEP **0802**, 080 (2008).
- [46] J. H. Kühn, F. Metzler and A. A. Penin, Nucl. Phys. B **795**, 277 (2008).
- [47] J. H. Kühn, F. Metzler, A. A. Penin, and S. Uccirati, JHEP **1106**, 143 (2011).
- [48] A. A. Penin and G. Ryan, JHEP **1111**, 081 (2011).

- [49] V. G. Gorshkov, V. N. Gribov, L. N. Lipatov and G. V. Frolov, Sov. J. Nucl. Phys. **6**, 95 (1968) [Yad. Fiz. **6**, 129 (1967)].
- [50] M. I. Kotsky and O. I. Yakovlev, Phys. Lett. B **418**, 335 (1998).
- [51] R. Akhoury, H. Wang and O. I. Yakovlev, Phys. Rev. D **64**, 113008 (2001).
- [52] A. Ferroglia, M. Neubert, B. D. Pecjak and L. L. Yang, Phys. Rev. Lett. **103** (2009) 201601.
- [53] E. Laenen, L. Magnea, G. Stavenga and C. D. White, JHEP **1101**, 141 (2011).
- [54] A. Banfi, P. F. Monni and G. Zanderighi, JHEP **1401**, 097 (2014).
- [55] T. Becher and G. Bell, Phys. Rev. Lett. **112**, 182002 (2014).
- [56] D. de Florian, J. Mazzitelli, S. Moch and A. Vogt, JHEP **1410**, 176 (2014).
- [57] C. Anastasiou, C. Duhr, F. Dulat, E. Furlan, T. Gehrmann, F. Herzog and B. Mistlberger, JHEP **1503**, 091 (2015).
- [58] A. A. Penin, Phys. Lett. B **745**, 69 (2015), Erratum: [Phys. Lett. B **771**, 633 (2017)].
- [59] A. A. Almasy, N. A. Lo Presti and A. Vogt, JHEP **1601**, 028 (2016).
- [60] A. A. Penin and N. Zerf, Phys. Lett. B **760**, 816 (2016), Erratum: [Phys. Lett. B **771**, 637 (2017)].
- [61] D. Bonocore, E. Laenen, L. Magnea, L. Vernazza and C. D. White, JHEP **1612**, 121 (2016).
- [62] R. Boughezal, X. Liu and F. Petriello, JHEP **1703**, 160 (2017).
- [63] I. Moulton, I. W. Stewart and G. Vita, JHEP **1707**, 067 (2017).
- [64] T. Liu, A. A. Penin and N. Zerf, Phys. Lett. B **771**, 492 (2017).
- [65] M. Beneke, M. Garny, R. Szafron and J. Wang, JHEP **1803**, 001 (2018).
- [66] R. Boughezal, A. Isgró and F. Petriello, Phys. Rev. D **97**, 076006 (2018).
- [67] R. Brüser, S. Caron-Huot and J. M. Henn, JHEP **1804**, 047 (2018).
- [68] I. Moulton, I. W. Stewart, G. Vita and H. X. Zhu, JHEP **1808**, 013 (2018).
- [69] M. A. Ebert, I. Moulton, I. W. Stewart, F. J. Tackmann, G. Vita and H. X. Zhu, JHEP **1812**, 084 (2018).
- [70] S. Alte, M. König and M. Neubert, JHEP **1808**, 095 (2018).
- [71] M. Beneke, M. Garny, R. Szafron and J. Wang, JHEP **1811**, 112 (2018).
- [72] M. Beneke, A. Broggio, M. Garny, S. Jaskiewicz, R. Szafron, L. Vernazza and J. Wang, JHEP **1903**, 043 (2019).
- [73] T. Engel, C. Gnendiger, A. Signer and Y. Ulrich, JHEP **1902**, 118 (2019).
- [74] M. A. Ebert, I. Moulton, I. W. Stewart, F. J. Tackmann, G. Vita and H. X. Zhu, JHEP **1904**, 123 (2019).
- [75] A. A. Penin, JHEP **2004**, 156 (2020).
- [76] M. Beneke, M. Garny, S. Jaskiewicz, R. Szafron, L. Vernazza and J. Wang, JHEP **2001**, 094 (2020).
- [77] Z. L. Liu and M. Neubert, arXiv:1912.08818 [hep-ph].
- [78] J. Wang, arXiv:1912.09920 [hep-ph].

- [79] M. Beneke and V. A. Smirnov, Nucl. Phys. B **522**, 321 (1998).
- [80] V. A. Smirnov, Phys. Lett. B **404**, 101 (1997).
- [81] V. A. Smirnov, *Applied asymptotic expansions in momenta and masses*, Springer Tracts Mod. Phys. **177**, 1 (2002).
- [82] D. R. Yennie, S. C. Frautschi and H. Suura, Annals Phys. **13**, 379 (1961).
- [83] C. Anastasiou, N. Deutschmann and A. Schweitzer, arXiv:2001.06295 [hep-ph].
- [84] S. Catani, Phys. Lett. B **427**, 161 (1998).
- [85] J. Frenkel and J. C. Taylor, Nucl. Phys. B **246**, 231 (1984).
- [86] R. V. Harlander, M. Prausa and J. Usovitsch, JHEP **1910**, 148 (2019).
- [87] M. Czakon and M. Niggetiedt, arXiv:2001.03008 [hep-ph].
- [88] J. Davies, R. Gröber, A. Maier, T. Rauh and M. Steinhauser, Phys. Rev. D **100**, 034017 (2019).
- [89] K. G. Chetyrkin, B. A. Kniehl and M. Steinhauser, Nucl. Phys. B **510**, 61 (1998).
- [90] Y. Schroder and M. Steinhauser, JHEP **0601**, 051 (2006).
- [91] K. G. Chetyrkin, J. H. Kuhn and C. Sturm, Nucl. Phys. B **744**, 121 (2006).
- [92] S. Catani, D. de Florian and M. Grazzini, JHEP **0105**, 025 (2001).
- [93] R. V. Harlander and W. B. Kilgore, Phys. Rev. D **64**, 013015 (2001).
- [94] C. Anastasiou, C. Duhr, F. Dulat, E. Furlan, T. Gehrmann, F. Herzog and B. Mistlberger, Phys. Lett. B **737**, 325 (2014).
- [95] F. Dulat, A. Lazopoulos and B. Mistlberger, Comput. Phys. Commun. **233**, 243 (2018).
- [96] H. Frellesvig, M. Hidding, L. Maestri, F. Moriello and G. Salvatori, arXiv:1911.06308 [hep-ph].
- [97] Z. L. Liu, B. Meca, M. Neubert and X. Wang, arXiv:2009.04456 [hep-ph].
- [98] Z. L. Liu, B. Meca, M. Neubert and X. Wang, arXiv:2009.06779 [hep-ph].
- [99] M. Niggetiedt, arXiv:2009.10556 [hep-ph].